AD-A106 228 NAVAL RESEARCH LAB WASHINGTON DC F/G 20/9
TILT AND SHIFT MODE STABILITY WITH LINE TYING.(U)
OCT 81 J M FINN, A REIMAN DE-01-81ET53020
UNCLASSIFIED NRL-MR-4610 NL

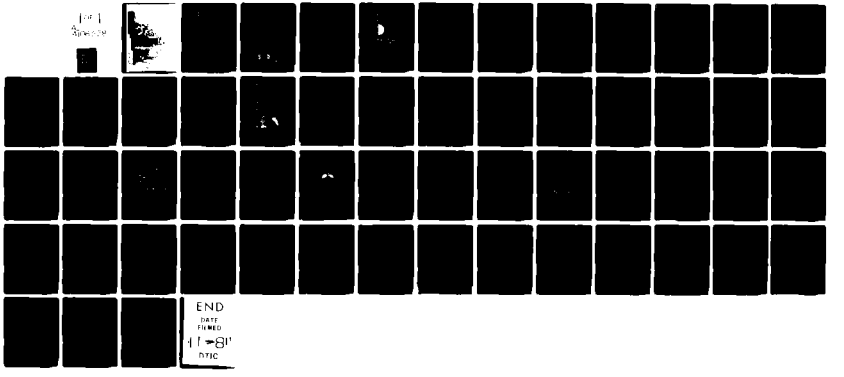

END
DATE FILMED
11-81
DTIC

SECURITY CLASSIFICATION OF THIS PAGE (When Data Entered)

REPORT DOCUMENTATION PAGE	READ INSTRUCTIONS BEFORE COMPLETING FORM
1. REPORT NUMBER: NRL Memorandum Report 4610	2. GOVT ACCESSION NO. / 3. RECIPIENT'S CATALOG NUMBER
4. TITLE (and Subtitle): TILT AND SHIFT MODE STABILITY WITH LINE TYING	5. TYPE OF REPORT & PERIOD COVERED: Interim report on a continuing NRL problem. / 6. PERFORMING ORG. REPORT NUMBER
7. AUTHOR(s): J. M. Finn and A. Reiman*	8. CONTRACT OR GRANT NUMBER(s)
9. PERFORMING ORGANIZATION NAME AND ADDRESS: Naval Research Laboratory, Washington, DC 20375	10. PROGRAM ELEMENT, PROJECT, TASK AREA & WORK UNIT NUMBERS: 47-0896-0-1
11. CONTROLLING OFFICE NAME AND ADDRESS: Department of Energy, Washington, DC 20545	12. REPORT DATE: October 23, 1981 / 13. NUMBER OF PAGES: 57
14. MONITORING AGENCY NAME & ADDRESS(if different from Controlling Office)	15. SECURITY CLASS. (of this report): UNCLASSIFIED / 15a. DECLASSIFICATION/DOWNGRADING SCHEDULE

16. DISTRIBUTION STATEMENT (of this Report)

Approved for public release; distribution unlimited.

17. DISTRIBUTION STATEMENT (of the abstract entered in Block 20, if different from Report)

18. SUPPLEMENTARY NOTES

*Present address: University of Maryland, College Park, MD 20742

This work was supported by the Department of Energy and the Office of Naval Research.

19. KEY WORDS (Continue on reverse side if necessary and identify by block number)

Spheromak
MHD instability
Tilt mode
Shift mode
Line tying

20. ABSTRACT (Continue on reverse side if necessary and identify by block number)

Magnetohydrodynamic stability of force free spheromak plasmas to n=1 free boundary tilt and radial shift modes is studied. The exterior region of open field lines is treated either as a conducting plasma or as a vacuum. In the former case the effect of line tying of the open field lines is present and is found to improve stability greatly. The equilibria which have optimum stability properties to the tilt and shift modes have a length to diameter ratio of 0.6, and can be stable with conducting walls at a relatively large distance.

DD FORM 1 JAN 73 1473 EDITION OF 1 NOV 65 IS OBSOLETE
S/N 0102-014-6601

SECURITY CLASSIFICATION OF THIS PAGE (When Data Entered)

CONTENTS

TILT AND SHIFT MODE STABILITY WITH LINE TYING

I. INTRODUCTION

A spheromak is a compact torus magnetic configuration whose toroidal and poloidal magnetic fields are produced by plasma currents confined by an external vertical field.[1] The advantages it shares with other compact torus designs are compactness and simplicity of design of external coils, walls and plasma, as well as a natural divertor. A plot of the flux surfaces of a typical spheromak configuration is shown in Fig. 1. Note the two classes of field lines, those on closed flux surfaces and the open field lines, separated by a surface we call the separatrix.

It has been found that a spheromak can be stable to internal modes if it is oblate.[1,2] Even an oblate spheromak requires an external conductor to stabilize the free-boundary modes. The question of how close the conducting shell must be and what shape it is allowed to take has an important bearing on spheromak experiments, and on the viability of proposed spheromak reactor designs. The moving ring field reversed reactor,[3] for example, would require a cylindrical shell, with the ends of the cylinder either far away or absent altogether. More conventional reactor designs would allow a shell which almost completely surrounds the plasma, but would nonetheless place constraints on how far the shell must be from the fusion plasma.

Manuscript submitted August 24, 1981.

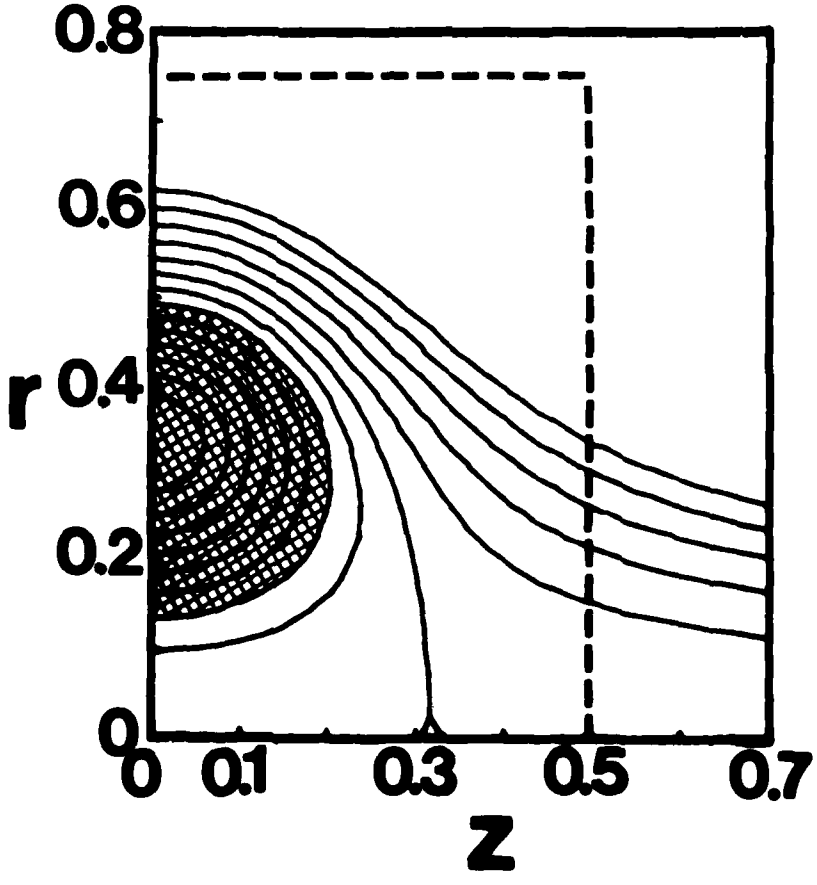

Fig. 1 — Flux surfaces of the most stable equilibrium. Currents flow in the shaded region. The dashed lines show one possible placement of the walls corresponding to marginal stability.

In this paper we numerically study wall stabilization of the external n = 1 magnetohydrodynamic (MHD) modes of the spheromak, with the effect of line tying due to plasma on the open field lines. Previous work indicates that the n = 1 modes are the most difficult of the external ideal MHD modes to stabilize.[4] The n = 1 tilt[5,6,7] and radial shift[5] modes have also been seen in spheromak experiments.

The first studies of MHD stability of spheromaks, using a nearly spherical equilibrium with $\nabla \times \underset{\sim}{B} = \mu \underset{\sim}{B}$ and μ constant, are due to Rosenbluth and Bussac.[2] They found that slightly prolate equilibria are unstable to an internal tilting mode, while slightly oblate equilibria require a shell of radius $R(1 - 0.2\epsilon)$ to stabilize the external tilting mode, where R is the plasma radius and ϵ is the ellipticity of the elliptical plasma surface. Later work by Finn et al.[8] and by Bondeson et al.[9] has shown that in a cylindrical conducting wall with endplates the internal tilt mode is unstable as long as the ratio of length to radius exceeds 1.67.

The existence of a q = 1 surface in the plasma (q is the usual safety factor) has been shown to be a destabilizing factor in oblate plasmas.[4] The equilibria studied in the present paper have q less than unity at the O-point and q decreasing toward the plasma edge, so that no such q = 1 surface exists. Our equilibria are force-free.

Tilting modes have been observed in several experiments to date, notably on the PS-1 device at the University of Maryland[5] and on plasmas produced by magnetized coaxial plasma guns at Los Alamos[6] and Livermore.[7] On the PS-1 experiment another n = 1 instability has also been observed, a radial shift mode.[5] (This should be distinguished from the axial shift, which is axisymmetric.)

The study described in this paper extends that of Rosenbluth and Bussac in considering more general separatrix shapes and in including two additional physical effects that turn out to be quite stabilizing. The first effect is that we consider equilibria whose current goes to zero smoothly at the separatrix, or even at an inner flux surface (so that there is a "flux hole"); i.e., $\mu = \mu(\psi)$. This smoothing of the current profile, which is almost certainly present in experiments, has an important stabilizing effect. This is plausible because a large part of the free energy for the free boundary tilt is due to the magnetic pressure imbalance at the perturbed X-point.

The second physical effect we include is line tying of the open field lines. That is, we consider the external region to be filled with conducting plasma (carrying zero equilibrium current) rather than vacuum. Since there is a normal component of magnetic field at the conducting walls (see Fig. 1), this effect is stabilizing. Note that

this configuration avoids a serious problem of conventional line-tied systems, that impurities can flow into the hot plasma from the metal wall. Although the closed field lines on which the equilibrium current flows are not themselves line-tied, we find that line tying of the open field lines greatly improves stability to n = 1 modes.

Recently, other groups have also performed stability computations on the tilt and radial shift modes.[10,11] The equilibrium models permitted a flux hole but did not permit finite current arbitrarily close to the separatrix. But the most important difference between this work and the work we present in this paper is our inclusion of the stabilizing effect of line tying of the open field lines. Our results without line tying (i.e., with a vacuum exterior) are consistent with the results of Refs. 10 and 11. (Exact comparison is difficult due to differences in profiles and wall shapes.) However, we find that the equilibria are considerably more stable with line tying. For example, one of our equilibria optimized for tilt and shift modes is marginally stable without line tying when the wall radius is 1.4 times the separatrix radius and the spacing between the axial walls is 1.1 times the separatrix length. With line tying, the last figure is 1.5.

In Section II we describe the equilibrium model, in particular the profiles and boundary conditions used.

In Section III we describe modified linear magnetohydrodynamic equations for force free plasmas and the time dependent code FFMHD that we use to integrate these equations of motion. We describe the special properties of the modified magnetohydrodynamic equations that make them particularly suitable to a system, such as the spheromak, that has magnetic neutral points (the X points on the symmetry axis). We also describe how the exterior region may be conveniently treated as a perfectly conducting plasma or a vacuum in this framework.

In Section IV we discuss the physical properties of the tilt and radial shift modes; in particular we show results from FFMHD pertaining to the stabilizing effect on the tilt mode of smoothing the current near the separatrix.

In Section V we describe in detail results obtained using FFMHD on the effect of elongation of the separatrix on the tilt and shift modes. There is an optimum elongation (separatrix half length to radius ratio), equal to about 0.6, nearly independent of other parameters. The optimum elongation without line tying is approximately the same, but the walls must be much closer to achieve stability. We also present marginal stability results in which we vary the elongation of the cylindrical wall. We find that line tying allows the axial wall to be removed

to a large distance, as required by the moving ring reactor scheme. We conclude that line tying in the radial wall is particularly stabilizing.

II. EQUILIBRIUM MODEL

Since the instabilities under consideration are current driven, we restrict our attention to force free equilibria, i.e., those equilibria having $\underset{\sim}{j} = \mu \underset{\sim}{B}$. However, we generalize the equilibria considered in Refs. 2, 8, and 9 by not requiring μ to be a constant in the plasma and by not requiring the separatrix to be nearly spherical. Instead, we keep only the obvious requirements that μ be constant on flux surfaces and go to zero continuously as the separatrix is approached from the inside.

From the general axisymmetric representation in cylindrical coordinates (r, θ, z)

$$\underset{\sim}{B} = \nabla\psi \times \nabla\theta + g(\psi)\nabla\theta \tag{1}$$

we conclude

$$\underset{\sim}{j} = \nabla \times \underset{\sim}{B}$$

$$= - \Delta^*\psi\nabla\theta + g'(\psi)\nabla\psi \times \nabla\theta \ , \tag{2}$$

where primes denote differentiation with respect to $\psi = rA_\theta$, the poloidal flux, and $\Delta^*\psi = r^2\nabla.(r^{-2}\nabla\psi)$. The requirement $\underset{\sim}{j} = \mu(\psi)\ \underset{\sim}{B}$ gives

$$\mu(\psi) = g'(\psi), \tag{3a}$$

$$\Delta^*\psi = - g(\psi)\ g'(\psi). \tag{3b}$$

The last equation is a specialization of the Grad-Shafranov equation to force free fields. We choose $\phi = \psi - \psi_h$, where $\psi_h < 0$ is the magnitude of the flux hole,

$$g(\psi) = aB_{\theta 0}\left\{\left[(\phi/\psi_0)^2 + \delta^2\right]^{\frac{1}{2}} - \delta\right\} \quad \text{for } \psi < 0, \qquad (4a)$$

$$= 0 \quad \text{for } \psi > 0, \qquad (4b)$$

where $\psi_0 < 0$ is the minimum of ψ, which occurs at the magnetic axis or 0-point; this model gives

$$\mu(\psi) = \frac{aB_{\theta 0}}{\psi_0^2} \frac{\phi}{\left[(\phi/\psi_0)^2 + \delta^2\right]^{\frac{1}{2}}} \quad \text{for } \psi < 0, \qquad (5a)$$

$$= 0 \quad \text{for } \psi > 0. \qquad (5b)$$

The boundary conditions are $\partial\psi/\partial z = 0$ at $z = 0$ (reflection symmetry), $\psi = 0$ at $r = 0$ (from $\psi = rA_\theta$) and the value of ψ as a function of z at $r = a$ (the radial wall), and as a function of r at $z = L$ (the endplate). The separatrix is given by $\psi = 0$. From (5) we see that the equilibrium current is zero on the open field lines ($\psi > 0$), that μ is nearly constant near $\psi = \psi_0$ and that μ is linear in ψ near the flux hole $[(\psi_h - \psi)/|\psi_0| \lesssim \delta]$. Notice that if $\delta = 0$, $\psi_h = 0$, the poloidal current is discontinuous at the separatrix. The specification of g as a function of the ratio ψ/ψ_0 as in (4) provides convergence of the iterative scheme used to solve (3b). See Ref. 12.

One set of boundary conditions at r = a and z = L, expressed in terms of dimensionless variables $\psi = \psi/(\frac{1}{2}B_0a^2)$ where B_0 is a reference field, is

$$\psi = r^2\left\{(1-.6\varepsilon)r_0^{-3} - (r^2 + z^2)^{-3/2}\right. \tag{6}$$
$$\left. + \varepsilon(4z^2 - r^2)\left[-.175r_0^{-5} - .425r_0^2(r^2 + z^2)^{-7/2}\right]\right\}.$$

For $|\varepsilon|<<1$, these boundary conditions, for $\delta = 0$, give the nearly spherical constant μ equilibria of Rosenbluth and Bussac,[2] with plasma surface given by $r = r_0(1 + \varepsilon \cos^2 \chi)$, where $\chi = \tan^{-1}(r/z)$. Equilibria with $\varepsilon > 0$ are prolate, and those with $\varepsilon < 0$ are oblate. Another set of boundary conditions that we use is

$$\psi = C_1r^2(1 + C_2z^2). \tag{7}$$

For this set of boundary conditions, equilibria with small C_1 have a separatrix which is near the wall. In fact, for $C_1 = \delta = 0$, the equilibria are those obtained analytically by Finn, Manheimer and Ott[8] and by Pondeson et al.[9] For $C_1 > 0$, the parameter C_2 controls the oblateness of the equilibrium by specifying the amount of flux passing through the radial wall r = a between z = 0 and z = L.

The flux surfaces ψ = const. of a typical equilibrium are shown in Fig. 1. Notice that the separatrix (separating

open field lines and those on closed flux surfaces) intersects the z-axis at magnetic neutral points, which we call X-points, one on each side of the plane of symmetry z = 0.

Our model (4) produces plasmas with fairly flat toroidal current profile. We observe that for all plasmas oblate enough to be stable to the internal tilting mode, the safety factor q is less than unity throughout the plasma. Therefore, for n = 1 modes no mode rational surfaces exist in the plasma. Furthermore, we do not expect that adding pressure with a fairly flat profile to a plasma with fixed separatrix will cause the safety factor q to go above unity.

III. MODIFIED MAGNETOHYDRODYNAMIC EQUATIONS

In this section we describe the modified magnetohydrodynamic equations of motion which are integrated in time by the numerical code FFMHD until the most unstable mode dominates. For more detail on the code, see Appendix A. The equation of motion for a force free equilibrium and ideal Ohm's law are

$$\rho\ddot{\xi} = \frac{1}{c}\mathbf{j}\times\mathbf{B} + \mathbf{j}\times\mathbf{B}, \tag{8a}$$

$$\mathbf{E} + \frac{1}{c}\dot{\xi}\times\mathbf{B} = 0, \tag{8b}$$

where ξ is the Eulerian plasma displacement, ρ is the density and dots denote derivation with respect to time. From (8) and Maxwell's equations, we conclude that the perturbed fields can be represented by a perturbed vector potential $\mathbf{A} = \xi\times\mathbf{B}$ and zero scalar potential. From (8a), therefore, we find

$$\rho\ddot{\mathbf{A}} = B^2\left[\mu(r)\,\mathbf{B} - \mathbf{j}\right]_\perp, \tag{9}$$

where $\perp$ represents components perpendicular to the unperturbed field $\mathbf{B}$. This is the basic equation of motion for the plasma which is integrated in time by the numerical code FFMHD. The Taylor stability[13] of equilibria with uniform μ was computed in Ref. 8 by integrating (9) without

the operation denoted by Λ; it was shown that Taylor stability of such equilibria is equivalent to ideal magnetohydrodynamic stability if no mode rational surfaces exist in the plasma.[8]

Because of the toroidal symmetry of the equilibrium ($\partial/\partial\theta = 0$), the cylindrical components of $\underset{\sim}{\xi}$ or of $\underset{\sim}{\xi}_A$ may be assumed to behave as $\exp(in\theta)$, where n is called the toroidal mode number.

For external or free boundary modes, integrating (9) to obtain $\underset{\sim}{\xi}_A$ rather than (8a) to obtain the displacement $\underset{\sim}{\xi}$ has a further advantage over those mentioned in Ref. 8 (for internal modes). As discussed in Ref. 2, a slightly oblate equilibrium can be unstable to tilting because the internal tilt motion is nearly marginally stable, and this motion produces a magnetic pressure imbalance across the perturbed X-points. This additional source of free energy drives the instability. Therefore, we might expect fairly singular behavior of $\underset{\sim}{\xi}$ near the X-points, since ξ_z should be large in that vicinity, but must be zero on the z-axis. (The latter property, which must hold for every vector with toroidal mode number $n \geq 1$, is discussed further in Appendix A.) The displacement plots shown in Fig. 2 show that this singular behavior is indeed found, and therefore that numerical problems would almost certainly be encountered in attempting to

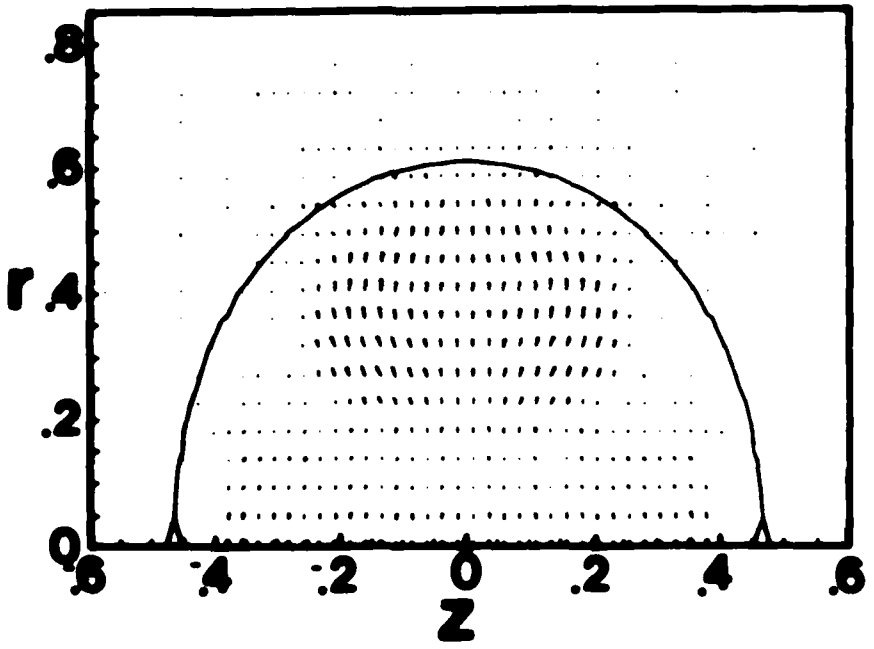

(a)

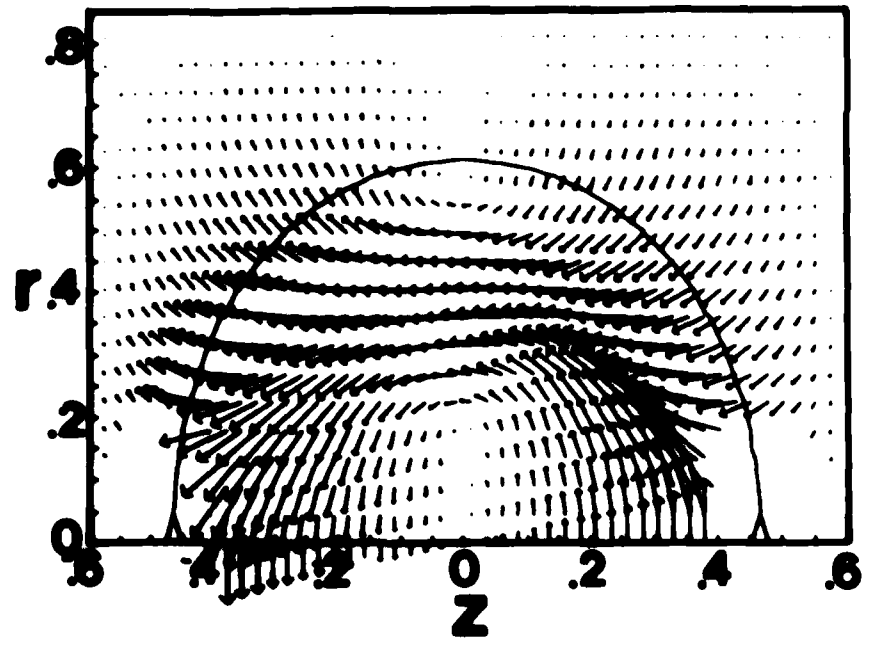

(b)

Fig. 2 — Poloidal displacement $\vec{\xi}$ for a tilt eigenmode. In (a), note that the real ($\cos\theta$) component of the tilt is shift-like. The imaginary ($\sin\theta$) component, shown in (b) clearly shows that effect of the magnetic pressure imbalance near the perturbed X-points.

integrate (8a). On the other hand, $\delta\underset{\sim}{A}$ is well behaved near the X-points, and no such numerical problems are observed in integrating (9). This property and the fact that no mode rational surfaces exist in the plasma allows us to use a simple cylindrical (r,z) grid rather than one matched to the flux surfaces of the equilibrium.

We have two optional ways of treating the exterior region of open field lines. The first, called the line tying option, is to treat the region as a perfectly conducting plasma carrying no equilibrium current. That is, since $\mu(\psi)$ is zero on the open field lines [c.f. equation (5)], we merely integrate (9) over the whole region without regard to the location of the separatrix. The boundary conditions $\hat{n} \times \delta\underset{\sim}{E} = 0$, $\hat{n} \cdot \underset{\sim}{\xi} = 0$ at the conducting impenetrable wall, together with the fact that $\hat{n} \cdot \underset{\sim}{B}$ is not zero imply $\underset{\sim}{\xi} = 0$ at the wall; this with the condition $\underset{\sim}{B} \cdot \delta\underset{\sim}{A} = 0$ yields the boundary condition on the vector potential $\delta\underset{\sim}{A} = 0$. Using this boundary condition it is easy to see that (9) has the usual energy principle, namely that the normal modes are extrema of

$$\omega^2 = \delta W/T \ , \tag{10}$$

where

$$\delta W = \frac{1}{2}\int\left[\delta\underset{\sim}{B}^2 - \mu(\psi)\,\delta\underset{\sim}{A} \cdot \delta\underset{\sim}{B}\right]d^3x \ , \tag{11a}$$

$$T = \frac{1}{2}\int(\rho/B^2)\,\delta\underset{\sim}{A}^2\, d^3x \tag{11b}$$

and where $\delta\underset{\sim}{A}$ satisfies the constraint $\underset{\sim}{B} \cdot \delta\underset{\sim}{A} = 0$. Using the toroidal symmetry of the equilibrium, we can write the toroidal dependence explicitly, i.e., $\delta\underset{\sim}{A} = \delta\underset{\sim}{A}^r \cos n\theta - \delta\underset{\sim}{A}^i \sin n\theta$, $\delta\underset{\sim}{B} = \delta\underset{\sim}{B}^r \cos n\theta - \delta\underset{\sim}{B}^i \sin n\theta$. Using these real variables in (10), (11) is equivalent to using the complex variables $\delta\underset{\sim}{A} = (\delta\underset{\sim}{A}^r + i\delta\underset{\sim}{A}^i)\exp(in\theta)$, $\delta\underset{\sim}{B} = (\delta\underset{\sim}{B}^r + i\delta\underset{\sim}{B}^i)$ $\exp(in\theta)$ with (10) but with

$$\delta W = \frac{1}{2}\int\left[|\delta\underset{\sim}{B}|^2 - \mu(\psi)\ \mathrm{Re}\ (\delta\underset{\sim}{A} \cdot \delta\underset{\sim}{B}^*)\right]d^3x\ , \qquad (12a)$$

$$T = \frac{1}{2}\int(\rho/B^2)\,|\delta\underset{\sim}{A}|^2\ d^3x\ ,$$

and $\underset{\sim}{B} \cdot \delta\underset{\sim}{A} = 0$.

The exterior plasma model includes the important stabilizing effect of line-tying of the open field lines. One way to see that this is a stabilizing influence is to note that having conducting plasma in the exterior region requires that the ideal magnetohydrodynamic flux constraint $\delta\underset{\sim}{B} = \nabla \times (\underset{\sim}{\xi} \times \underset{\sim}{B})$ or $\delta E_{||} = 0$ holds throughout the region, while this is not the case if the exterior region is vacuum. Also recall that the boundary condition $\delta\underset{\sim}{A}_t = 0$, together with (8a) and $\underset{\sim}{j} = \mu\underset{\sim}{B}$ implies that the total plasma displacement $\underset{\sim}{\xi}$ is zero at the wall. (If the wall is a flux surface, only the normal component of $\underset{\sim}{\xi}$ must be zero.) As we shall discuss further, the boundary conditions when the conducting wall surrounds a vacuum are $\hat{n} \times \delta\underset{\sim}{A} = 0$,

regardless of whether a normal component of the equilibrium field exists. In Appendix B we establish more rigorously the stabilizing effect of line tying.

Various different normalizations, i.e., models for the density $\rho(r,z)$ are possible. The choice affects growth rates but not, of course, marginal stability. The simplest such model has ρ = const. Another model which is very useful has $B^2/\rho = v_A^2$ = const. (the Alfvén speed). Whereas this model has the unphysical effect of allowing equilibrium density variations along the field lines, it has the advantage of producing growth rates of the order of three times those of the constant density model. This advantage is due to the fact that the density goes to zero at the X-points, where a large destabilizing contribution occurs. Any model having $\rho = \rho(\psi)$ and with small density near the X-points would have a very large Alfvén speed v_A near the separatrix and would therefore have a very stringent Courant condition. For more details see Appendix A. Of course, the unphysical nature of the second model has no effect on the marginal stability computations. We expect that the growth rates for a system whose density decreases monotonically to a finite value at the separatrix would be bounded by the growth rates of our two extreme models.

The alternative model for the exterior region is a vacuum. The usual energy principle treatment[14] of the vacuum is to minimize the vacuum contribution to δW,

$$\delta W_v = \int (\nabla \times \underset{\sim}{\delta A})^2 \, d^3x, \tag{13}$$

that is satisfy $\nabla \times \nabla \times \underset{\sim}{\delta A} = 0$, subject to the boundary conditions $\hat{n} \cdot \underset{\sim}{\xi} \, \underset{\sim}{B} = - \hat{n} \times \underset{\sim}{\delta A}$ at the plasma-vacuum interface and $\hat{n} \times \underset{\sim}{\delta A} = 0$ at the conducting wall. Then, stability is determined by minimizing

$$\omega^2 = \delta W / T, \tag{14}$$

where δW consists of the plasma contribution (11a) plus δW_v and where T is still given by (11b) or $\frac{1}{2}\int \rho \underset{\sim}{\xi}^2 d^3x$. Our method, using the time dependent code FFMHD, is to integrate (9) on the closed flux surfaces and, on the open field lines, to integrate

$$\rho \delta \ddot{A} = - B^2 \left[\underset{\sim}{\delta j} - \exp(-p\psi) \, \underset{\sim}{\delta j}_{||} \right], \tag{15}$$

where p is an adjustable parameter and $||$ denotes components parallel to $\underset{\sim}{B}$. Clearly the total differential equation (9), (15) is continuous across the separatrix $\psi = 0$. Far from the separatrix, specifically when the exponential factor in (15) is negligible, (15) reduces to the form of the equation of motion without the constraint $\underset{\sim}{B} \cdot \underset{\sim}{\delta A} = 0$. We

generally pick p large so that there is only a very small region immediately outside the separatrix where the exponential factor in (15) is nonnegligible. There are cases, in fact, in which p can be so large that the exponential factor is negligible at every grid point in the exterior region. However, occasionally it is necessary to use a more moderate value of p to avoid numerical instabilities.

Taking the exponential factor in (15) to be zero, we easily see that equations (9), (15) have an energy principle represented by $\omega^2 = \delta W/T'$, where δW consists of the same plasma and vacuum terms as in (14) but where

$$T' = \int_P (\rho/B^2)\, \delta\underset{\sim}{A}_\perp^2\, d^3x + \int_V (\rho/B^2)\, \delta\underset{\sim}{A}^2\, d^3x. \qquad (16)$$

Here, the notation serves to emphasize the fact that $\underset{\sim}{B} \cdot \delta\underset{\sim}{A} = 0$ inside the plasma, but that no such constraint exists in the vacuum. In Appendix B we show that the condition that $\hat{n} \times \delta\underset{\sim}{A}$ be continuous across the separatrix (equivalent to $\hat{n} \cdot \underset{\sim}{\xi}\, \underset{\sim}{B} = -\hat{n} \times \delta\underset{\sim}{A}$) is indeed satisfied by (9), (15) even when $\exp(-p\psi)$ is taken to be zero. The density ρ in the vacuum is, of course, fictitious; however δW consists of the same two terms as the conventional energy principle and therefore predicts marginal stability correctly. In principle, this fictitious density could be made small in order to compute actual growth rates, but the resulting

large Alfvén speed would produce a very stringent Courant condition.

There are two other features of the code FFMHD worth discussing. The first is that we generally add an additional term $\gamma_0^2 \rho \delta\underset{\sim}{A}$ to the right hand side of the equations of motion (9) in the case of plasma exterior and (9), (15) in the case of vacuum exterior. This modification speeds up convergence, i.e., the evolution to a pure normal mode, if only one unstable mode exists. In this case the optimum value of γ_0 is $|\omega_2|$, where ω_2 is the frequency of the second normal mode, the mode with the second largest eigenvalue $-\omega^2$. If two unstable normal modes exist, or if the second mode has $\omega \underset{\sim}{>} 0$, this additional term does not help. Indeed, we have observed that when a $q = 1$ surface exists in the plasma, where q is the usual safety factor, the convergence rate to $n = 1$ instabilities is not aided by having finite γ_0, presumably because continuum eigenfunctions with $\omega^2 \underset{\sim}{>} 0$ exist. However, throughout this paper we deal with short (oblate) plasmas where $q < 1$ throughout the plasma. In addition, in cases for which no unstable normal mode exists, using γ_0 enables us to compute the normal mode with smallest ω^2.

The other noteworthy feature of the code is that we compute growth rates, for the purpose of extrapolation to marginal stability, by (10) rather than merely observing the

exponential growth rate directly after a pure mode is obtained. We call the former growth rate γ_n and the latter γ_t. That is, our code is essentially an energy principle code where the optimum trial function is obtained by integrating the modified equations of motion. Our expectation that the growth rates γ_n computed by this method will be more accurate is based on Rayleigh's principle, namely that the error in the eigenvalue computed by a variational principle is of the order of the square of the error (e.g., grid errors) in the eigenfunction. On the other hand, the growth rate γ_t observed directly in the code should have errors of the same order as the eigenfunction. We have performed convergence tests with increasingly finer grids in r,z and we have always found that γ_n is more accurate. For more detail see Appendix A.

Computing growth rates γ_n by (10) also allows us to run for shorter times, since a first order error in the eigenfunction due to incomplete convergence to the most unstable normal mode leads only to second order errors in the growth rate. This property also holds for γ_t if the growth rate is computed by observing the e-folding rate of T (11b), because of orthogonality. This property does not hold for any other quadratic form. However, the errors in this method of computing the growth rate become amplified near marginal stability if γ_0 is finite. It is

easily shown that the error in γ_t relative to γ_0 becomes first order in the error in the eigenfunction near marginal stability. The error in γ_t relative to γ_t itself is, of course, even larger.

IV. TILT AND SHIFT MODES

In this section we present numerical studies of the stability of free boundary n = 1 modes with line tying on the open field lines. We restrict this study to oblate equilibria because prolate equilibria are unstable to internal tilt modes. For the equilibria we consider (4), the safety factor q is below unity throughout the plasma, and therefore the rather singular behavior near the q = 1 surface typical of internal kink modes[4,9] does not occur.

As we have discussed in a different context in Sec. III, a free boundary tilt motion may be unstable with walls fairly close to the plasma because the nearly marginal internal tilt motion produces a magnetic pressure imbalance across the perturbed X-points. A modification of the displacement $\underset{\sim}{\xi}$ to take advantage of this free energy can provide $\delta W<0$, i.e., instability.[2] In fact, the method of Rosenbluth and Bussac[2] of computing stability of equilibria with uniform μ is based on computing this magnetic pressure imbalance. However, their method does not generalize to $\mu(\psi)$ in any obvious way.

The poloidal displacement $\underset{\sim}{\xi}_p = \xi_r \hat{r} + \xi_z \hat{z}$ of a tilt mode in a typical equilibrium is shown in Figure 2. (The displacement is computed from the growing solution $\delta\underset{\sim}{A}$ of (9) by $\underset{\sim}{\xi} = \underset{\sim}{B} \times \delta\underset{\sim}{A}/B^2$.) Notice that the imaginary part of $\underset{\sim}{\xi}$, i.e., the sin θ Fourier component is indeed a nearly

rigid rotation together with an inward motion at the rotated X-point. The real part, i.e., the cos θ component, is a nearly rigid radial shift.

Our general procedure for studying stability for a given equilibrium is to fix the position of the radial wall $r = r_w$ and perform several stability runs with the axial wall $z = z_w$ successively closer. We then extrapolate to marginal stability. The square of the growth rate $\gamma_n^2 = -\omega^2$ from (10) is usually quite linear near marginal stability.

Typical growth rates found for tilting modes with normalization $v_A^2 = B^2/\rho$ = const. have $\gamma L/v_A \sim 1$. For $B \sim$ 2 kg, $n \sim 10^{14}$ and $L \sim 50$ cm, as in the Los Alamos experiment, we find $\gamma \sim 10^6$ sec^{-1}. As we have discussed earlier, with the ρ = const. normalization, this is lower by a factor of order 3.

Constant μ equilibria of Ref. 2, i.e., with (4), $\delta = 0$, $\psi_h = 0$, with boundary conditions (6) with $\varepsilon \lesssim 0$ required a tight fitting shell. For example for $\varepsilon = -0.4$, with the radial wall nearly touching the separatrix at the midplane $r_w = r_s$, marginal stability occurs when the axial wall nearly touches the separatrix at the X-point, i.e., $z_w = z_s$. This is in qualitative agreement with the results of Ref. 2, namely that a spherical wall must be at $(r^2 + z^2)^{1/2} = r_s(1 + .2|\varepsilon|)$ for marginal stability. Of course, qualitative agreement is all we expect since our

wall is cylindrical rather than spherical and since $\varepsilon = -0.4$ is not small enough in absolute value for the treatment of Ref. 2 to be accurate.

In Figure 3 we show z_w, the position of the axial wall required for stability as a function of δ, the parameter of (4), (5) that determines the smoothing of the poloidal current (which is discontinuous if $\delta = 0$) near the separatrix. The radial wall was nearly touching the separatrix, $r_w/r_s = 1.01$. The stability, as measured by z_w, improves dramatically with δ. Notice that the point z_s where the separatrix intersects the z-axis (at the X-points) decreases with δ, because the total current decreases. This stabilization due to smoothing the current in the neighborhood of the separatrix is plausible, because the destabilizing force, namely the pressure imbalance at the X-points, is localized near the separatrix.

In Figure 4 we show the axial wall position z_w required for stability, for $r_w/r_s = 1.01$ and $\delta = 0.15$, as a function of the elongation parameter ε of (6). Note that there is a dramatic improvement with oblateness that begins around $\varepsilon = -.15$. Improvement for large $|\varepsilon|$ is reasonable, since the results of Ref. 8 show that the energy of the $n = 1$ internally tilted equilibrium continues to rise relative to the axisymmetric state as the plasma length decreases, until extremely short plasmas are obtained. It is worth mentioning here that there are no instances in which z_w

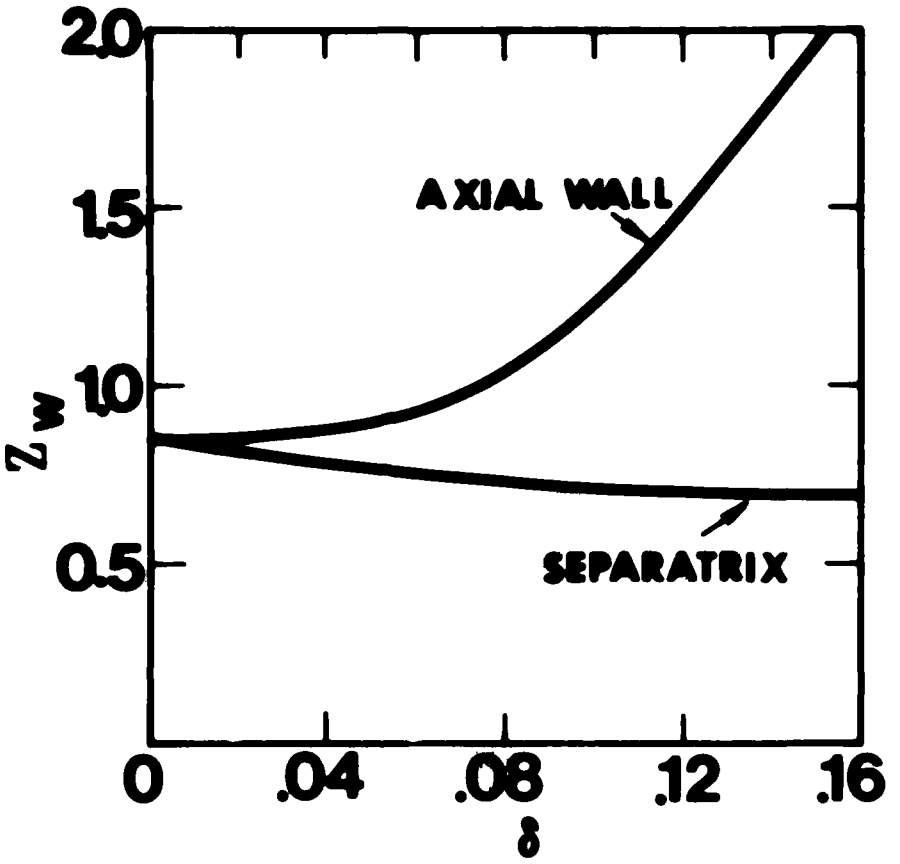

Fig. 3 — Position of axial wall required for stability to tilt and separatrix position as a function of the current smoothing parameter δ of eqs. (4), (5); $\epsilon = -0.4$.

must be less than z_s, i.e., the axial wall intersecting the separatrix, to stabilize external tilting modes, even though having z_w slightly less than z_s would still leave quite a large exterior region. his is probably due to the fact that the displacement of the boundary is large in a neighborhood of the X-point on the z-ε is This feature is illustrated in Figure 4, where $z_w = z_s$ is required for marginal stability over a fairly large range of ε, $-0.5 < \varepsilon < 0$, even though z_s is decreasing with $|\varepsilon|$.

The results shown in Figures 3 and 4 illustrate well the stabilizing influence of current smoothing and oblateness. However, we should emphasize that the radial wall was touching the separatrix, that the separatrix had only modest oblateness, and that line tying was present, i.e., the exterior region was plasma. In the next section we present studies of stability of the tilt mode with walls further removed with and without line tying.

When our equilibria are made more oblate (i.e., larger $|\varepsilon|$) than those shown in Figure 4, a new instability, the radial shift mode, appears.[15] From Figure 5, we see that the real part (i.e., cos θ Fourier component) of the poloidal displacement $\underset{\sim}{\xi}_p$ is roughly a rigid radial shift of the plasma. The imaginary part of $\underset{\sim}{\xi}_p$ (the sin θ component) is again tilt-like. One way to understand the appearance of this instability for more oblate plasmas is

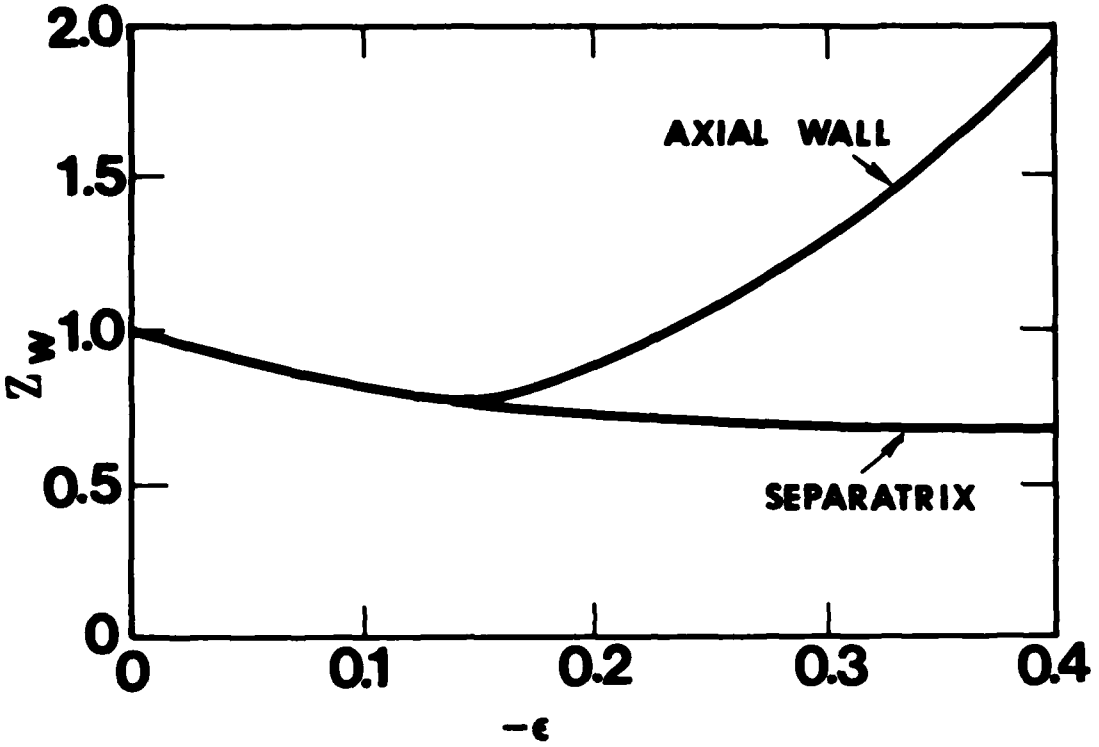

Fig. 4 — Position of axial wall required for stability to tilt and separatrix position as a function of oblateness parameter ϵ; $\delta = 0.15$.

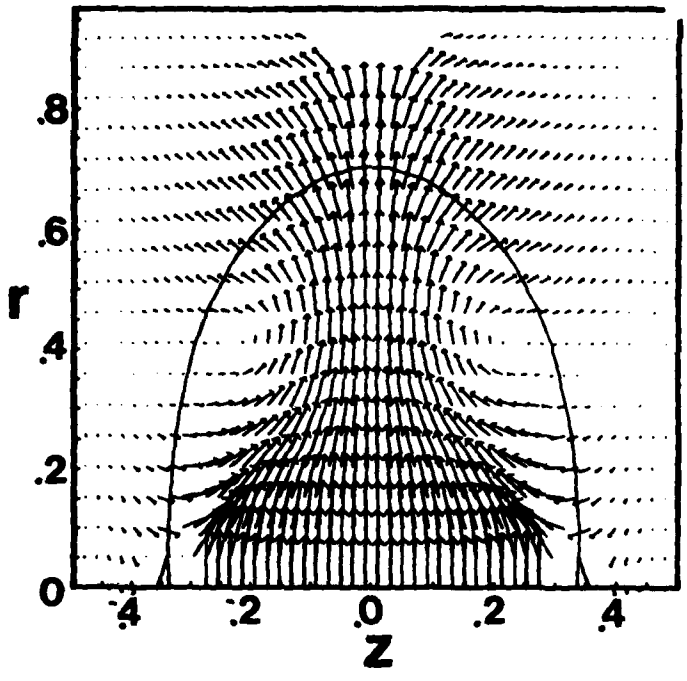

(a)

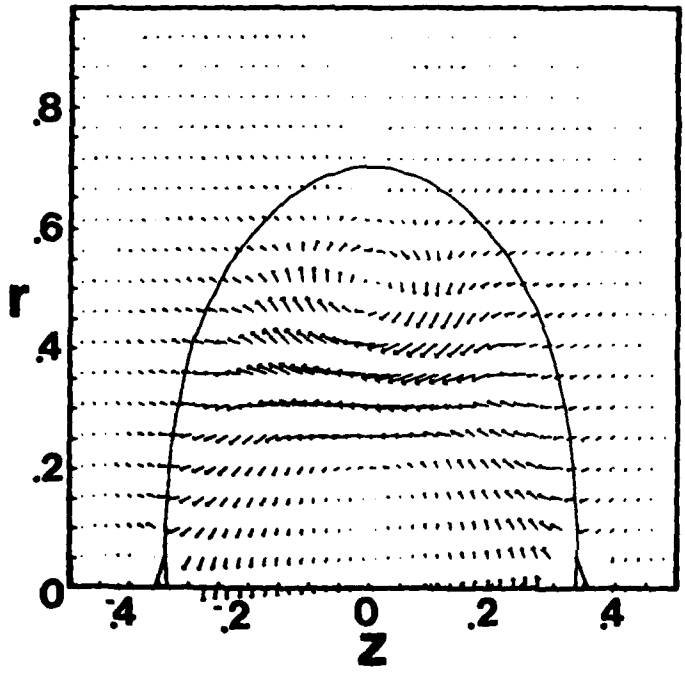

(b)

Fig. 5 — Poloidal displacement $\underset{\sim}{\xi}$ for a shift eigenmode. The real ($\cos\theta$) component shown in (a) shows again the effect of magnetic pressure imbalance near the perturbed X-points. The imaginary ($\sin\theta$) component shown in (b) is somewhat tilt-like.

to note that oblate plasmas are produced from boundary conditions (6) or (7) by increasing the amount of (negative) flux passing through the radial wall, i.e., by increasing $\partial^2\psi/\partial z^2$ at r = a. This is achieved by decreasing ε in (6) or by increasing c_2 in (7). Thus, for $\partial^2\psi/\partial z^2 > 0$, the Grad-Shafranov equation (3b) with $g(\psi) = 0$ implies $r\,\partial/\partial r\left[(1/r)\,\partial\psi/\partial r\right] < 0$ or $\partial Bz/\partial r < 0$, that is that the field index is negative. On this basis, we might expect a radial instability like the radial precession mode in Astron type geometries.[16] The simplest model for this instability applies to a rigid ring of current so weak that its self forces are negligible. For this model instability occurs if $B_z(Ne)^2/4\pi Mc\ I + \nu < 0$, where Ne is the total charge of the current carrying species, M is the total ring mass, I is the current carried by the ring and $\nu = rB_z'/B_z$ is the (external) field index. (The first term in this inequality is in essence a finite Larmor radius effect and may be neglected if the Larmor radius is small or if dissipation is present.[16])

A related approach to understanding the shift instability is to note that very oblate equilibria are confined radially by strong magnetic fields away from the midplane z = 0 but by rather weak fields near the midplane, so that even a stable rigid shift motion may have a weak restoring force, i.e., be nearly marginally stable. However, such a

shift produces magnetic pressure imbalance at the perturbed X-points, which can be strong enough to destabilize the mode. This mechanism is closely related to the mechanism by which the external tilt in oblate plasmas is destabilized.[2] The inward displacement in response to this pressure imbalance is clearly evident in Figure 5.

V. OPTIMUM PARAMETERS FOR STABILITY

In this section we present results of a systematic search for optimum parameters for stability to both the tilt and the shift mode. We have performed these studies using both models for the exterior region, namely plasma exterior (i.e., with line tying) and vacuum exterior.

In Section IV we studied the behavior as a function of δ, the current smoothing parameter, and found that stability as measured by the position of the axial wall required for marginal stability, improved monotonically with δ. For $\psi_h = 0$, this behavior has a plateau at about $\delta = .25$.

In Figure 6 we show the axial wall position required for marginal stability as a function of separatrix shape with $\psi_h = 0$ for $\delta = .15$ and $\delta = .25$. On the vertical axis is the ratio z_w/z_s, where z_w is the position of the axial wall and z_s is the position of the X-point, where the separatrix intersects the z-axis. On the horizontal axis is the shape parameter, the ratio of half length to radius z_s/r_s (=1 for a spherical separatrix). Both sets of runs were done with line tying and with the position of the radial wall relative to the radial position of the separatrix r_w/r_s fixed at 1.25. Note that in both cases stability is optimal for $z_s/r_s \approx 0.6$. The equilibrium with $\delta = .25$ is clearly more stable than that with $\delta = .15$. We have also

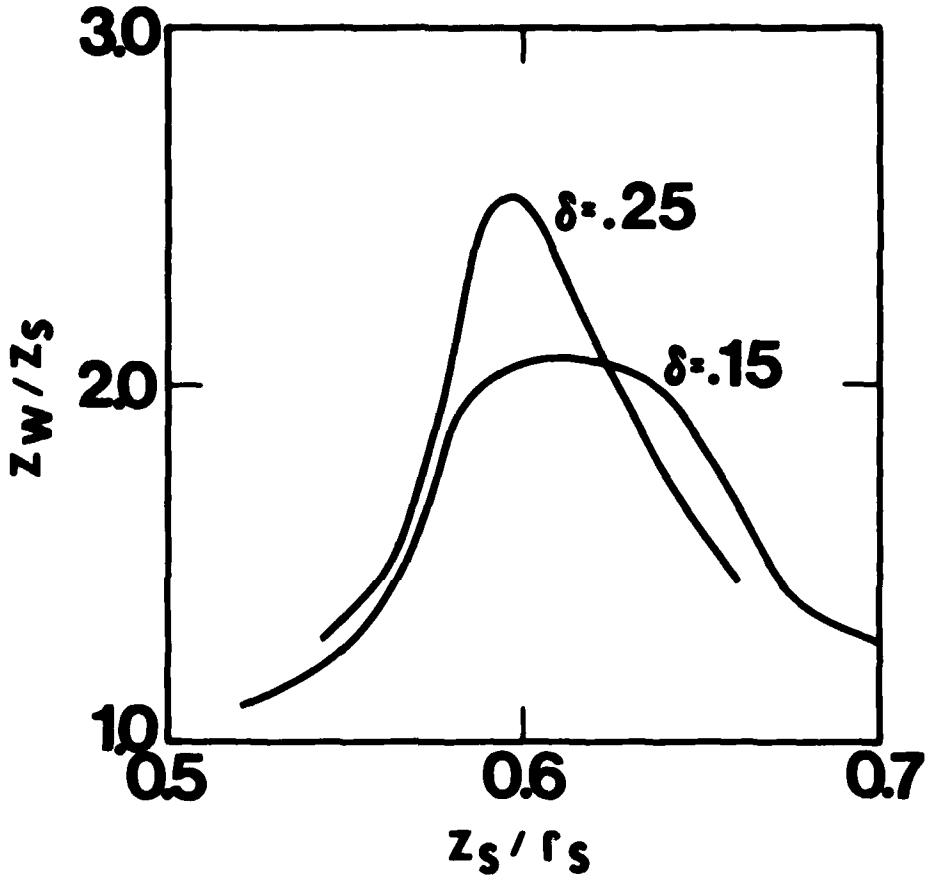

Fig. 6 — Axial position of wall required for stability (relative to separatrix half length) as a function of the elongation parameter z_s/r_s, with $\psi_h = 0$, $r_w/r_s = 1.25$, and $\delta = 0.15, 0.25$, with line tying. For plasmas longer than the optimum $z_s/r_s \approx 0.6$, the most unstable mode is the tilt; otherwise it is the shift.

done a set of runs with $\delta = .35$, and have found that the marginal stability points with line tying lie very close to the $\delta = .25$ plot shown in Figure 6.

Figure 7 shows the stability for $\psi_h = 0$, and $\delta = .25$ both with and without line tying. The plot with line tying is just the same as the $\delta = .25$ curve shown in Figure 6. Without line tying, stability is again optimal at roughly $z_s/r_s = 0.6$. Clearly, line tying greatly improves the stability. In this case, with our fixed radial wall, the axial wall is permitted to be about nine times further from the separatrix with line tying than without.

For Figure 8 we have taken the equilibrium corresponding to optimal stability with line tying in Figure 7 ($r_0 = .99999$ and $\varepsilon = -8.2$ in equation 6), and have determined the radial wall position required for marginal stability as a function of the axial wall position. Note again that line tying greatly improves the stability. These results indicate that, in the presence of line tying, the radial wall alone may be sufficient to stabilize the $n = 1$ modes. Our code does not, of course, allow us to verify this directly, because we require a finite number of axial grid points. In any case, it is clear that line tying does allow us to remove the axial wall to a large distance, as required by the moving-ring reactor scheme.[3]

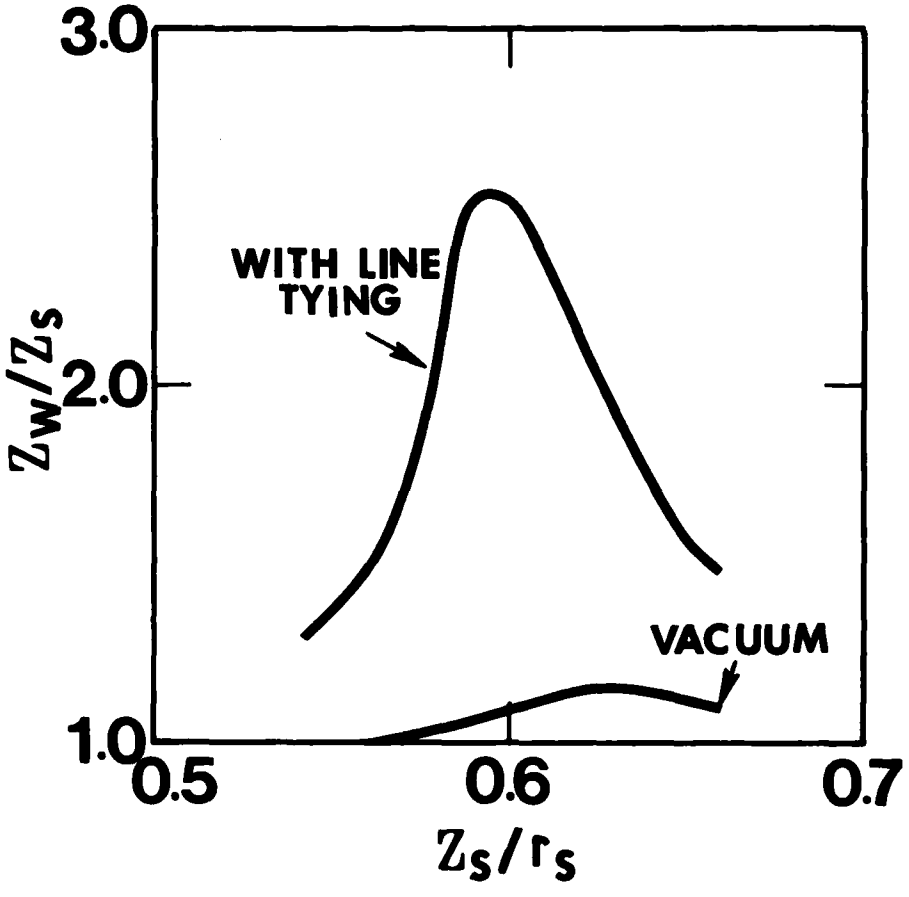

Fig. 7 — Axial position of the wall required for stability as a function of elongation with and without line tying; $\psi_h = 0$, $\epsilon = 0.25$, and $r_w/r_s = 1.25$.

The results shown in Figure 8 show clearly that when the axial wall is removed to a large distance, line tying in the radial wall is responsible for stability.

Finally, we have looked at the effect on stability of a flux hole. Our results with current smoothing near the separatrix suggest that the introduction of a flux hole should be stabilizing, and we find that that is indeed the case. Again, our results make sense if we recall that the displacement near the X-point plays an important role in destabilizing both the tilt and the shift mode.

Figure 9 shows axial wall position required for marginal stability plotted against separatrix shape, with $\psi_h = .2$, $\delta = .05$, and $r_w/r_s = 1.4$. The optimally shaped equilibrium is somewhat more stable than in Figure 8, where $\psi_h + \delta$ has the same value but $\psi_h = 0$. Now, because the surface of our current carrying equilibrium plasma lies somewhat inside the separatrix, the wall is actually somewhat further away from the plasma than indicated by our plot. This can be seen in Figure 1, which shows the equilibrium corresponding to optimal stability with line tying in Figure 9 ($C_1 = 0.25$ and $C_2 = 6.0$ in equation 7). Equilibrium currents flow only in the shaded region, with the dashed lines showing the position of the walls at marginal stability. Once again, line tying greatly improves the stability. The results of our runs for these equilibria

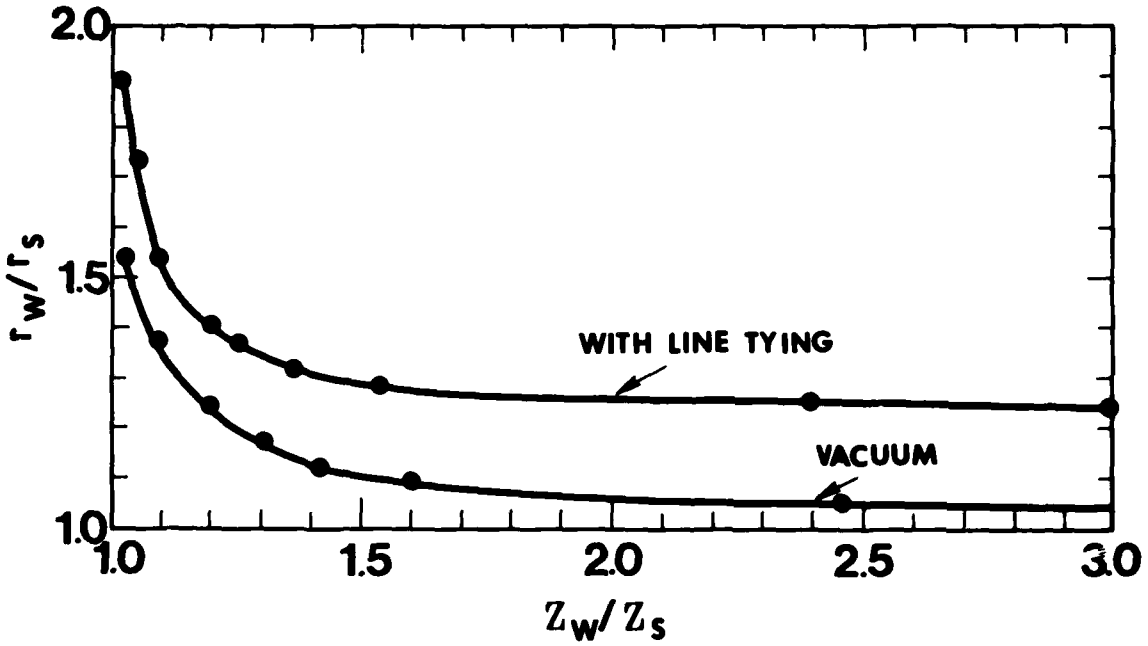

Fig. 8 — Axial position of wall *vs.* radial position at marginal stability, both scaled to the relevant separatrix dimension; $\delta = 0.25$, $\epsilon = -8.2$ ($z_s/r_s = 0.59$). Results are shown with and without line tying of the open field lines.

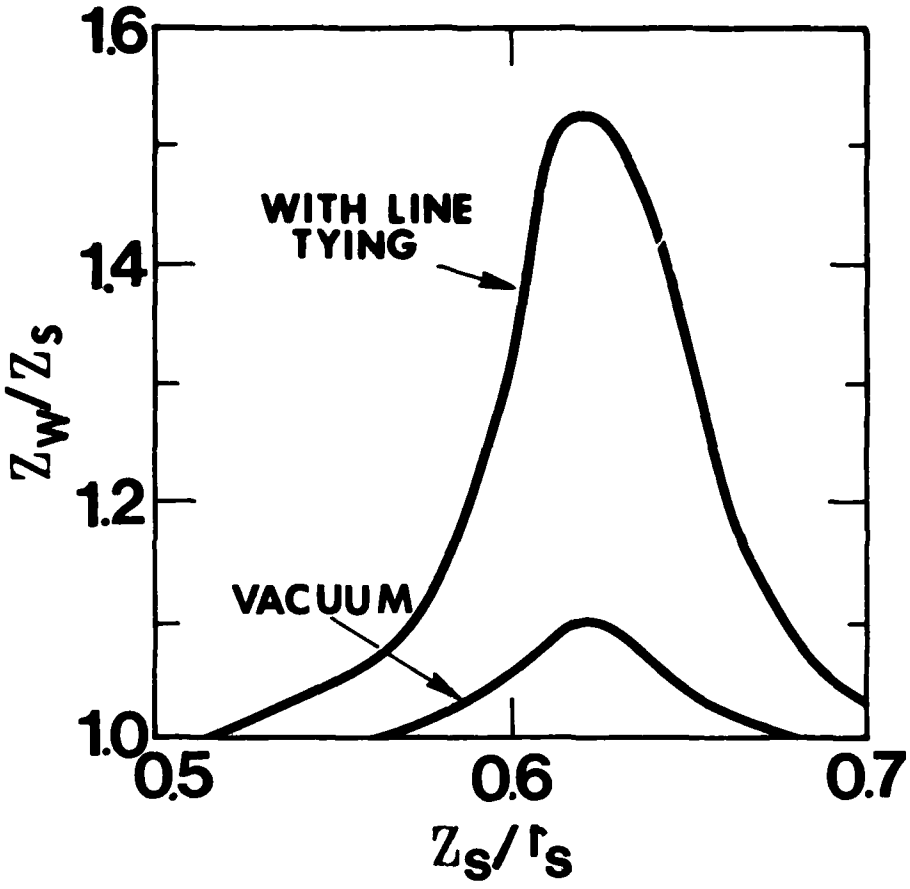

Fig. 9 — Axial wall position required for stability as a function of elongation with and without line tying; $\psi_h = 0.2$, $\delta = 0.05$, and $r_w/r_s = 1.4$.

without line tying are consistent with the results obtained by others for similar equilibria.[10,11,15] (For comparison with the results of other authors, we caution that the wall radius is sometimes expressed as the distance of the wall to the plasma, $\psi = \psi_h$, relative to the minor plasma radius. In this normalization, the radial wall of Figure 9 is a distance of approximately 1.2 from the plasma, and the maximum distance of the axial wall without line tying is about .8.)

Note that in Figure 8, with $r_w/r_s = 1.4$, the marginal position of the axial wall for the equilibrium without a flux hole is given by $z_w/z_s \tilde{>} 1.2$. Comparing with Figure 9, we see that the flux hole allows us to move the walls further from the separatrix, this despite the fact that the surface of the current distribution has moved inside the separatrix.

VI. SUMMARY

Our tool for studying the stability of force free spheromak equilibria to the current driven tilt and radial shift modes is the time dependent magnetohydrodynamic code FFMHD. This code integrates the perturbed vector potential $\delta\underset{\sim}{A}(= \underset{\sim}{\xi} \times \underset{\sim}{B})$ in time rather than the displacement $\underset{\sim}{\xi}$. For this reason it is well suited to the treatment tilt and radial shift modes, whose displacement can be singular at the magnetic neutral points (X-points) on the axis of symmetry. The external region may either be treated as a vacuum or as a conducting plasma with zero equilibrium current. Equilibria treated by the latter model are generally more stable due to line tying of the open field lines.

We find that nearly spherical "Taylor equilibria," having $\nabla \times \underset{\sim}{B} = \mu\underset{\sim}{B}$ with μ uniform require a tightly fitting cylindrical wall for stability, even with line tying. For equilibria whose current goes to zero more smoothly near the separatrix, and with a conducting plasma in the exterior region, the walls may be removed a considerable distance.

The optimum plasma shape for stability to both the tilt and the radial shift modes has ratio of half length to radius 0.6, nearly independent of other equilibrium parameters. With line tying on the open field lines, the radial and axial walls can be removed from the plasma by at least 50 percent, relative to the total radius and length

of the separatrix. The axial wall may be removed to at least several times the plasma length with the radial wall at a distance of over 1.2 times the plasma radius. These results are summarized in Figure 8. With vacuum on the open field lines, the optimum shape is about the same, but the walls must be considerably closer.

ACKNOWLEDGMENTS

We wish to thank E. Ott, W. Manheimer, L. Sparks, S. Jardin, H. Dalhed, and J. Hammer for illuminating discussions.

This work was supported by the Department of Energy and the Office of Naval Research.

APPENDIX A: NUMERICAL CODE

The numerical code FFMHD integrates (9) throughout the region enclosed by the walls or (9), (15), depending upon whether the exterior is modeled by a conducting plasma or a vacuum (possibly with a small matching region). The finite difference equations used are based upon the simplest central differences for derivatives with respect to t, r, and z. Errors are of order Δt^2, Δr^2, Δz^2. The Courant condition which one might expect for such a scheme, when $B^2/\rho = v_A^2 = \text{const.}$, is $\Delta t < \min(\Delta r, \Delta z)/v_A$. Empirically, we find that a slightly smaller time step is required for numberical stability. For the alternate normalization $\rho = \text{const.}$, the required time step is about 20 percent smaller (where v_A now represents the maximum Alfvén speed). As discussed in Section III, we expect that a model with low density in the exterior region [in order to obtain correct growth rates with (16)] would require extremely short time steps.

The boundary conditions on the perturbed vector potential $\delta\underset{\sim}{A}$ at the conducting walls have been discussed in Section III. Boundary conditions are also required on the symmetry axis r = 0 because of the coordinate singularity.

We describe the boundary conditions at r = 0 for each toroidal mode number n separately. Assuming the components δA_x, δA_y, δA_z to be analytic in x, y, z, i.e., expanding for fixed z

$$\begin{aligned} \delta A_x &= A + Bx + Cy + \cdots, \\ \delta A_y &= D + Ex + Fy + \cdots, \\ \delta A_z &= H + Ix + Jy + \cdots, \end{aligned} \tag{A1}$$

we find

$$\begin{aligned} \delta A_r &= \tfrac{1}{2}(B + F)r + A\cos\theta + D\sin\theta \\ &\quad + \tfrac{1}{2}(B - F)r\cos 2\theta + \tfrac{1}{2}(C + E)r\sin 2\theta + \cdots, \\ \delta A_\theta &= \tfrac{1}{2}(E - C)r + D\cos\theta - A\sin\theta \\ &\quad + \tfrac{1}{2}(E + C)r\cos 2\theta + \tfrac{1}{2}(F - B)r\sin 2\theta + \cdots, \\ \delta A_z &= H + I\,r\cos\theta + J\,r\sin\theta + \cdots. \end{aligned} \tag{A2}$$

As in Section III, we write $\underset{\sim}{\delta A} = \mathrm{Re}\left[(\underset{\sim}{\delta A}^r + i\underset{\sim}{\delta A}^i)\exp(in\theta)\right]$ $= \underset{\sim}{\delta A}^r \cos n\theta - \underset{\sim}{\delta A}^i \sin n\theta$. For n = 0 we conclude A = D = 0 and therefore $\delta A_r^r = \delta A_\theta^r = 0$. (Imaginary parts are automatically zero.) Also, since the neglected terms of δA_z are $O(r^2)$, we have $(\partial/\partial r)\delta A_z^r = 0$.

For $n = 1$, we find $B + F = B - F = 0$, $C + E = C - E = 0$, so that $(\partial/\partial r)\delta A_r = (\partial/\partial r)\delta A_\theta = 0$ for real and imaginary parts and $\delta A_r^r = \delta A_\theta^i$, $\delta A_r^i = -\delta A_\theta^r$. We also find $\delta A_z^r = \delta A_z^i = 0$.

For $n = 2$ we find $\delta A_r \sim \delta A_\theta \sim r$ as $r \to 0$ and $\delta A_z \sim r^2$ as $r \to 0$. It is easy to see that for $n \geq 2$ this generalizes to $\delta A_r \sim \delta A_\theta \sim r^{n-1}$, $\delta A_z \sim r^n$.

The conditions for $n = 0$ are easily implemented in the code. Similarly, for $n \geq 2$, it is adequate to set all three components of $\delta\underset{\sim}{A}$ equal to zero at $r = 0$. For $n = 1$ the issue is complicated by the fact that the conditions given overdetermine δA_r and δA_θ at $r = 0$, and implementing any subset of these conditions leads to numerical instability. We were able to overcome these difficulties by setting δA_r^r and δA_θ^i both equal to the average of the values of δA_r^r and δA_θ^i obtained by using the conditions $(\partial/\partial r)\delta A_r^r = (\partial/\partial r)\delta A_\theta^i = 0$. The analogous procedure was used for δA_r^i and δA_θ^r.

When the code is run with the option that initial conditions are generated in the code, we insure that the initial conditions obey the boundary conditions at $r = 0$ as well as those at the conducting wall. (The other option, which speeds up convergence to the most unstable mode, is to input the vector potential from a previous run.)

The typical grid we use to integrate the finite difference form of (9) or (9),(15) has 40 or 50 points radially and 100 points axially. We have performed

convergence tests on finer grids (up to 70 x 170) and conclude that the relative grid error in $\gamma_n = (-\delta W/T)^{\frac{1}{2}}$ is less than three percent. In the same set of runs the improvement in the accuract of γ_t (see Section III) was much more pronounced. In the transient phase, i.e., for short times, energy is conserved in the code to within a few percent (the change in total energy relative to the change in kinetic energy) for a 40 x 100 grid and to within a fraction of a percent for a 70 x 170 grid. By the time an unstable normal mode has evolved, energy conservation is worse. We trace this behavior to singular behavior near the X-points. However, in no cases that we have tested does this reflect itself in poor accuracy for γ_n.

APPENDIX B: EXTERIOR REGION MODELS

Our purpose here is to explain in more detail various properties of our modified magnetohydrodynamic equations in the exterior region. Specifically, we prove that normal modes of (9),(15) have continuous tangential components of $\delta\underset{\sim}{A}$, and that the model with plasma exterior is more stable than the one with vacuum exterior because of line tying.

We first prove that regular (i.e., bounded) normal modes of the system with a vacuum exterior described by (9),(15) have continuous tangential components $\hat{n} \times \delta\underset{\sim}{A}$ at the separatrix, even when the exponential factor in (15) is zero. We identify three components of the perturbed vector potential at the separatrix $\delta\underset{\sim}{A}_n$, $\delta\underset{\sim}{A}_{t1}$, and $\delta\underset{\sim}{A}_{t2}$. These are, respectively, the normal component, the tangential component parallel to $\underset{\sim}{B}$, and the tangential component perpendicular to $\underset{\sim}{B}$. We also split the curl operator into tangential and normal components, so that $\delta\underset{\sim}{B} = \nabla \times \delta\underset{\sim}{A} = \delta\underset{\sim}{B}_n + \delta\underset{\sim}{B}_t$, where $\delta\underset{\sim}{B}_n = \nabla_t \times \delta\underset{\sim}{A}_t$, and $\delta\underset{\sim}{B}_t = \nabla_t \times \delta\underset{\sim}{A}_n + \nabla_n \times \delta\underset{\sim}{A}_t$. We also find $\delta\underset{\sim}{j} = \nabla \times \delta\underset{\sim}{B} = \delta\underset{\sim}{j}_n + \delta\underset{\sim}{j}_t$, where $\delta\underset{\sim}{j}_n = \nabla_t \times \nabla_t \times \delta\underset{\sim}{A}_n + \nabla_t \times \nabla_n \times \delta\underset{\sim}{A}_t$ and $\delta\underset{\sim}{j}_t = \nabla_t \times \nabla_t \times \delta\underset{\sim}{A}_t + \nabla_n \times \nabla_t \times \delta\underset{\sim}{A}_n + \nabla_n \times \nabla_n \times \delta\underset{\sim}{A}_t$. Therefore the normal mode equations (9),(15), with B^2/ρ constant for convenience, and near the separatrix where $\mu(\psi)$ can be neglected, are

$$\gamma^2 \delta \underset{\sim}{A}_n = - \delta \underset{\sim}{j}_n \qquad \text{(B1)}$$

$$\gamma^2 \delta \underset{\sim}{A}_{t2} = - \delta \underset{\sim}{j}_{t2} \qquad \text{(B2)}$$

$$\delta \underset{\sim}{A}_{t1} = 0 \quad \text{for } \psi < 0 \qquad \text{(B3)}$$

$$\gamma^2 \delta \underset{\sim}{A}_{t1} = - \delta \underset{\sim}{j}_{t1} \quad \text{for } \psi > 0$$

Now, for contradiction, assume $\delta \underset{\sim}{A}_{t2}$ is discontinuous at $\psi = 0$. Then, from (B2), either $\delta \underset{\sim}{A}_{t2}$ must behave like $\delta'(\psi)$ or $\delta \underset{\sim}{A}_n$ must behave as $\delta(\psi)$. Both of these conclusions contradict the assumption that $\delta \underset{\sim}{A}$ is bounded, so that $\delta \underset{\sim}{A}_{t2}$ is continuous. Next, assume that $\delta \underset{\sim}{A}_{t1}$ is discontinuous at $\psi = 0$. Then, from (B1) and since $\delta \underset{\sim}{A}_{t2}$ is continuous, we see that $\delta \underset{\sim}{A}_n$ must behave as $\delta(\psi)$, which is again a contradiction. Therefore the tangential components of $\delta \underset{\sim}{A}$ are continuous at $\psi = 0$. Incidentally, a similar argument cannot be applied to prove the continuity of the normal component of $\delta \underset{\sim}{A}$, because the only normal derivative of $\delta \underset{\sim}{A}_n$, in $\delta \underset{\sim}{j}_t$, is balanced by a <u>second</u> normal derivative of $\delta \underset{\sim}{A}_t$. The fact that the system (9),(15) requires continuity of $\delta \underset{\sim}{A}_t$ but allows discontinuity of $\delta \underset{\sim}{A}_n$ explains why FAMHD has no numerical problems when run in the exterior vacuum mode, even when the exponential factor in (15) is so small that it is essentially zero on every grid point in the

exterior region. Also, it is easy to see that the above proof does not require that B^2/ρ be constant, or even that ρ be continuous at $\psi = 0$. (Note that if we pick the fictitious density ρ so that $v_A^2 = c^2$ in the exterior region, then (15) merely states that $\nabla \times \delta\underset{\sim}{B}$ is balanced by the displacement current in the exterior, and therefore that the perturbed current is zero.)

In the previous paragraph we have completed the proof that the system (9),(15) has identical magnetohydrodynamic stability properties as the physical system with vacuum on the open field lines, since it has the same contributions to δW in plasma and in vacuum [c.f. (11)] and since the usual boundary condition $\hat{n} \times \delta\underset{\sim}{A} = n \times (\underset{\sim}{\xi} \times \underset{\sim}{B}) = - \hat{n} \cdot \underset{\sim}{\xi}\, \underset{\sim}{B}$ holds. We now turn to a proof that the system described by alternate equations of motion (9), with a plasma on the open field lines, is more stable than the system with vacuum exterior. This stabilizing influence is due to the fact that we have a normal component of the equilibrium field $\underset{\sim}{B}$ at the walls, i.e., we have line tying. Indeed, it is shown in Ref. 8 that if $\hat{n} \cdot \underset{\sim}{B} = 0$ at the walls, and if no mode rational surface exists in the plasma, the condition $\underset{\sim}{B} \cdot \delta\underset{\sim}{A} = 0$ can always be satisfied by a gauge transformation.

The remaining question is whether the additional constraints on the vector potential in the exterior plasma model, namely $\underset{\sim}{B} \cdot \delta\underset{\sim}{A} = 0$ and continuity of $\delta\underset{\sim}{A}_n$ at the separatrix, are physical constraints (i.e., constraints on the fields) or whether they can be imposed by a gauge transformation. If we try to impose the former condition, i.e., try to satisfy $\underset{\sim}{B} \cdot \nabla\chi + \underset{\sim}{B} \cdot \delta\underset{\sim}{A} = 0$, we find

$$\chi = C - \int_0^{\ell} \delta\underset{\sim}{A} \cdot d\underset{\sim}{\ell} \tag{B4}$$

where the integral is along a field line and C is the value of χ at the wall (this must be a constant by the condition that the tangential component of $\delta\underset{\sim}{A}$ in both gauges must vanish at the wall). Therefore, for any field line that passes through the walls twice (see Figure 1) we must have $\int \delta\underset{\sim}{A} \cdot d\underset{\sim}{\ell} = 0$. For n = 0 (axisymmetric) modes this means that the perturbed toroidal flux $\oint \delta\underset{\sim}{B} \cdot \hat{n} dA$ between any two flux surfaces ψ = const. in the exterior region must be zero. For modes with $n \neq 0$ we have, from Appendix A, $\delta A_z = 0$ on the axis r = 0. Therefore the perturbed toroidal flux enclosed by the z-axis and any flux surface ψ = const. that intersects the walls must be zero. Therefore the constraint $\underset{\sim}{B} \cdot \delta\underset{\sim}{A} = 0$ is a physical constraint and has a stabilizing influence. As an aside, we comment that any closed flux surfaces in the flux hole $\psi > \psi_h$

[c.f. equation (4)] may be considered to be in vacuum or to contain plasma. For such flux surfaces, with $B_\theta = 0$, the condition $\underset{\sim}{B} \cdot \delta\underset{\sim}{A} = 0$ can be imposed by a gauge transformation only if the integral over the closed field line $\oint \delta\underset{\sim}{A} \cdot d\underset{\sim}{\ell} = 0$. Since this implies that the perturbed toroidal flux is zero within the flux surface, having plasma on the closed field lines in the flux hole is also stabilizing. (This is a special case of the theorem of Reference 8, that the constraint $\underset{\sim}{B} \cdot \delta\underset{\sim}{A} = 0$ is stabilizing if a mode rational surface—here $q = 0$—exists.)

Finally, the boundary condition on $\delta\underset{\sim}{A}_n$ is a further physical constraint. Indeed, let us require that the same gauge function of (B.4) satisfy $\partial\chi/\partial n = (\delta A_p - \delta A_v) \cdot \hat{n}$ at $\psi = 0$, where $\partial\chi/\partial n$ is the normal derivative, $\delta\underset{\sim}{A}_p = \underset{\sim}{\xi} \times \underset{\sim}{B}$ is the vector potential inside the plasma ($\psi < 0$) and $\delta\underset{\sim}{A}_v$ is the vacuum vector potential. We find from (B4)

$$\oint \delta\underset{\sim}{A} \cdot d\underset{\sim}{\ell} = - \Delta\hat{n} \cdot \delta\underset{\sim}{A}_p \ , \qquad \text{(B5)}$$

$$= \Delta |\underset{\sim}{B}| \xi_\theta \ .$$

The integral on the left is over a curve consisting of the z-axis exterior to the plasma and part of the separatrix up to the point in question, and returning on a nearby field line, separated by a distance Δ at the terminal point on the separatrix. Thus, the continuity boundary condition

on $\delta A_{\nu n}$ imposes a physical constraint on the flux through the area bounded by this curve, and is therefore also stabilizing.

REFERENCES

1. M.N. Bussac, H.P. Furth, M. Okabayaski, M.N. Rosenbluth, and A.M.M. Todd, in Plasma Physics and Controlled Nuclear Fusion Research (International Atomic Energy Agency, Vienna, 1979), p. 249.
2. M.N. Rosenbluth and M.N. Bussac, Nucl. Fusion 19, 489 (1979).
3. A.C. Smith, G.A. Carlson, H.H. Fleischmann, W. Grossman, T. Kammash, K.R. Schultz and D.M. Woodall, Proceedings of the Third Symposium on the Physics and Technology of Compact Toroids, Los Alamos (1980), p. 12.
4. P. Gautier, R. Gruber, and F. Troyon, to be published.
5. H. Bruhns, Y. Chong, G. Goldenbaum, G. Hart, and R. Hess, Proceedings of the Third Symposium on the Physics and Technology of Compact Toroids, Los Alamos (1980), p. 97.
6. I. Henins, H. Hoida, T. Jarboe, R. Linford, J. Marshall, K. McKenna, D. Platts, and A. Sherwood, Ibid, p. 101.
7. W. Turner, G. Goldenbaum, E. Granneman, C. Hartman, D. Prono, J. Paska, and A. Smith, Ibid, p. 113.
8. J.M. Finn, W.M. Manheimer and E. Ott, to appear in Phys. Fluids.
9. A. Bondeson, G. Marklin, Z. An, H.H. Chen, Y.C. Lee, and C.S. Liu, to appear in Phys. Fluids.

10. M.S. Chance, R.L. Dewar, R.C. Grimm, S.C. Jardin, J.L. Johnson, and D.A. Monticello, Proceedings of the Third Symposium on the Physics and Technology of Compact Toroids, Los Alamos (1980), p. 56.

11. H.E. Dalhed, Ibid, p. 60.

12. L. Sparks, J.M. Finn and R.N. Sudan, Phys. Fluids 23, 611 (1980).

13. J.B. Taylor, Phys. Rev. Lett. 33, 1139 (1974).

14. I.B. Bernstein, E.A. Frieman, M.D. Kruskal, and R.M. Kulsrud, Proc. Roy. Soc. London Ser. A244, 17 (1958).

15. S.C. Jardin, M.S. Chance, R.L. Dewar, J.L. Johnson and D.A. Monticello, Bull. Am. Phys. Soc. 25, 861 (1980).

16. J.M. Greene and B. Coppi, Phys. Fluids 8, 1745 (1965); H.P. Furth, Phys. Fluids 8, 2020 (1965).

DISTRIBUTION LIST

DOE
P.O. Box 62
Oak Ridge, Tenn. 37830

UC20 Basic List (116 copies)
UC20f (192 copies)
UC20g (176 copies)

NAVAL RESEARCH LABORATORY
Washington, D.C. 20375

Code 4700 (26 copies)
Code 4790 (150 copies)

DEFENSE TECHNICAL INFORMATION CENTER
Cameron Station
5010 Duke Street
Alexandria, VA 22314 (2 copies)


FILME